

Conformational Isomerism in Triosmium Clusters: Structures of Yellow and Red $\text{Os}_3(\text{CO})_{11}[\text{P}(p\text{-C}_6\text{H}_4\text{F})_3]$ and $\text{Os}_3(\text{CO})_{11}(\text{P}^t\text{Bu}_3)$

Valerie M. Hansen,[†] Andrew K. Ma,[†] Kumar Biradha,[‡]
Roland K. Pomeroy,^{*,†} and Michael J. Zaworotko[‡]

Department of Chemistry, Simon Fraser University, Burnaby, British Columbia, Canada V5A 1S6, and Department of Chemistry, Saint Mary's University, Halifax, Nova Scotia, Canada B3H 3C3

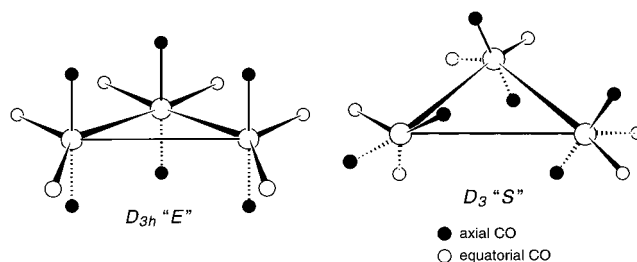
Received May 11, 1998

The clusters $\text{Os}_3(\text{CO})_{11}(\text{PR}_3)$ ($\text{R} = p\text{-C}_6\text{H}_4\text{F}$, **1**; Bu^t , **2**) have been prepared by the addition of PR_3 to $\text{Os}_3(\text{CO})_{11}(\text{CH}_3\text{CN})$, and their structures determined. There are yellow and red forms of **1** (**1y** and **1r**, respectively). The structure of **1y** has the typical structure for $\text{Os}_3(\text{CO})_{11}(\text{PR}_3)$ (PR_3 = phosphine or phosphite) complexes with the axial carbonyls perpendicular to the Os_3 triangle, whereas in **1r** the individual $\text{Os}(\text{CO})_3(\text{L})$ ($\text{L} = \text{CO}, \text{PR}_3$) units are twisted with respect to each other such that neighboring carbonyls on adjacent Os atoms are in a staggered configuration. The reason for the twisting in **1r** is believed to be due to intermolecular edge-to-face interactions between fluorophenyl rings in the solid. In solution **1** is yellow with spectroscopic properties typical of $\text{Os}_3(\text{CO})_{11}(\text{PR}_3)$ compounds. Unlike **1y** and its analogues, **2** is deep red both in the solid and in solution. The structure of **2** reveals that like **1r** it also has the twisted structure. It is believed that the large size and strong donor properties of the P^tBu_3 ligand destabilize the edge-bridging molecular orbitals in **2** such that the twisted form, which is sterically favored, is adopted. Consistent with this view is that the Os–Os bond cis to the P^tBu_3 in **2** is long, at 2.9416(3) Å; in **1y** and **1r** the corresponding lengths are 2.872(1) and 2.888(1) (two independent molecules in the unit cell of **1y**) and 2.9117(4) Å, respectively.

Introduction

The structures of $\text{M}_3(\text{CO})_{12}$ ($\text{M} = \text{Ru}, \text{Os}$) consist of a triangular metal skeleton with six equatorial and six axial carbonyl ligands.^{1,2} The axial carbonyls on neighboring metal atoms are eclipsed to one another, giving the molecules D_{3h} symmetry (Chart 1). For reasons discussed below we designate $\text{M}_3(\text{CO})_{11}(\text{L})$ (L = two-electron donor ligand) complexes based on the D_{3h} form of the parent carbonyl as the “E” conformer. The eclipsed arrangement is not the most favored conformation from steric considerations. Lauher has calculated that the D_3 conformer (Chart 1) of $\text{Ru}_3(\text{CO})_{12}$ with adjacent axial carbonyls in a staggered orientation should be some 3.0 kcal mol^{−1} more stable than the D_{3h} conformer in the absence of electronic factors.³ We label $\text{M}_3(\text{CO})_{11}(\text{L})$ clusters based on the D_3 version of $\text{M}_3(\text{CO})_{12}$ as the “S” form. As Lauher pointed out, an $\text{M}(\text{CO})_4$ unit is isolobal with CH_2 that has two frontier orbitals (a_1 and b_1), and three such groups should bind with strict D_{3h} symmetry. Twisting of the $\text{M}(\text{CO})_4$ units with respect to each other to give the sterically preferred D_3 form would destroy this favorable overlap.³ Molec-

Chart 1



ular orbital calculations on D_{3h} $\text{Fe}_3(\text{CO})_{12}$ and $\text{Ru}_3(\text{CO})_{12}$ support this view.^{4,5}

Derivatives of the type $\text{M}_3(\text{CO})_{11}(\text{PR}_3)$ (i.e., $\text{M} = \text{Ru}, \text{Os}$, not Fe) usually have close to E structures (i.e., based on the D_{3h} conformation).^{6–11} The distortion toward the

[†] Simon Fraser University. E-mail address: pomeroy@sfu.ca.

[‡] Saint Mary's University.

(1) Churchill, M. R.; Hollander, F. J.; Huthchinson, J. P. *Inorg. Chem.* **1977**, *16*, 2655.

(2) Churchill, M. R.; DeBoer, B. G. *Inorg. Chem.* **1977**, *16*, 878.

(3) Lauher, J. W. *J. Am. Chem. Soc.* **1986**, *108*, 1521.

(4) Schilling, B. E. R.; Hoffmann, R. *J. Am. Chem. Soc.* **1979**, *101*, 3456.

(5) Delley, B.; Manning, M. C.; Ellis, D. E.; Berkowitz, J.; Troglor, W. C. *Inorg. Chem.* **1982**, *21*, 2247.

(6) Deeming, A. J. In *Comprehensive Organometallic Chemistry II*; Abel, E. W.; Stone, F. G. A.; Wilkinson, G., Eds.; Pergamon: Oxford, U.K., 1995; Vol. 7, Chapter 12, p 683.

(7) Cullen, W. R.; Rettig, S. J.; Zhang, H. *Can. J. Chem.* **1996**, *74*, 2167. For structures of $\text{Ru}_3(\text{CO})_{11}(\text{PR}_3)$ compounds published before 1995 see ref 6, Table 1 and references therein.

(8) Bruce, M. I.; Liddell, M. J.; Hughes, C. A.; Skelton, B. W.; White, A. H. *J. Organomet. Chem.* **1988**, *347*, 157.

(9) Ehrenreich, W.; Herberhold, M.; Süß-Fink, G.; Klein, H.-P.; Thewalt, U. *J. Organomet. Chem.* **1983**, *248*, 171.

(10) Benfield, R. E.; Johnson, B. F. G.; Raithby, P. R.; Sheldrick, G. M. *Acta Crystallogr.* **1978**, *B34*, 666.

S configuration can be measured by the C(ax)–M–M–C(ax) dihedral angles. Bruce and co-workers found these angles ranged from close to 0° to 16.8° (in Os₃(CO)₁₁[PPh(OMe)₂]) in the five Os₃(CO)₁₁(PR₃) structures determined at the time; in similar Ru compounds this dihedral angle was as high as 24.4° (in Ru₃(CO)₁₁–[P(OCH₂)₃CET]).⁸ In the more highly substituted clusters, M₃(CO)_{12–x}(PR₃)_x (*x* = 2, 3), the twisting is even more significant, with a maximum value for the C(ax)–M–M–C(ax) dihedral angle of 44.8° in Ru₃(CO)₁₀–(PPh₃)₂.¹² Twisting to give a *D*₃-type conformation is also found in Os₃(CO)₆[P(OMe)₃]₆.¹³

In unpublished work, we have prepared over 20 clusters of the type Os₃(CO)₁₁(PR₃) in order to ascertain the effect of the R group on the barriers to carbonyl nonrigidity that these molecules exhibit in solution.¹⁴ With the exception of one form of Os₃(CO)₁₁[P(*p*-C₆H₄F)₃] and the PBu₃ analogue, the clusters are yellow or orange. Crystal structures of the yellow and orange Os₃(CO)₁₁(PR₃) compounds by ourselves and others show a geometry based on Os₃(CO)₁₂ with one of the equatorial carbonyls replaced by the phosphorus ligand; that is, the syn axial carbonyls are in an approximate eclipsed (*E*) orientation.^{6,8–10,14} Here we describe the structures of the two exceptions (which are red) that reveal that they have the twisted *S* conformation, that is, with the syn axial carbonyls staggered with respect to each other. We also report the structure of two yellow forms of Os₃(CO)₁₁[P(*p*-C₆H₄F)₃] that have the common *E* configuration.

Experimental Section

Unless otherwise stated, manipulations of starting materials and products were carried out under a nitrogen atmosphere with the use of standard Schlenk techniques. Hexane was refluxed over potassium, distilled, and stored over molecular sieves before use; dichloromethane was dried in a similar manner except that CaH₂ was employed as the drying agent. The precursory compound, Os₃(CO)₁₁(CH₃CN), was prepared by a literature procedure.¹⁵ NMR spectra were recorded on a Bruker AMX400 spectrometer at the appropriate operating frequencies for ¹H, ¹³C, and ³¹P nuclei.

Preparation of Os₃(CO)₁₁[P(*p*-C₆H₄F)₃] (1) and Os₃(CO)₁₁(PBu₃) (2). A solution of Os₃(CO)₁₁(CH₃CN) (50 mg, 0.054 mmol) and P(*p*-C₆H₄F)₃ (26 mg, 0.081 mmol) in CH₂Cl₂

(25 mL) was stirred at room temperature for 15 min. The solvent was removed on the vacuum line and the residue chromatographed on a silica gel column (1 × 20 cm) with hexane/CH₂Cl₂ (9:1) as the eluant. The desired product was isolated as the second (yellow) band and recrystallized from hot hexane to give **1** in ~50% yield. The PBu₃ analogue, **2**, was prepared in a similar manner except that a 5-fold excess of the phosphine was employed and the reaction required 18 h to go to completion (as indicated by IR spectroscopy). The first product eluted in the chromatographic separation was identified as Os₃(CO)₁₂; a second yellow band that has not been identified was then eluted; the third orange-red band was the desired product (the yield was ~30%); a fourth yellow band was also not identified. Os₃(CO)₁₁[P(*p*-C₆H₄F)₃]: mp (red form) 167–168 °C; (yellow form) 168.5–169.5 °C (turning orange ~70–110 °C); UV–vis (hexane) 29,100 (ε_M × 10^{–4} = 9.81), 24 500 (5.29) cm^{–1}; IR (hexane) ν(CO) 2110 (w), 2057 (m–s), 2036.5 (m), 2022 (s), 2004 (vw), 1994 (w), 1981 (w), 1969 (vw), 1959.5 (vw) cm^{–1}; ¹H NMR (CD₂Cl₂) δ 7.50–7.39 (m), 7.21–7.16 (m); ³¹P{¹H} NMR (CD₂Cl₂) δ –3.6; ¹³C{¹H} NMR (CD₂Cl₂/CH₂Cl₂ 1:4; –53 °C) δ 193.2 (2C, *J*_{PC} = 8.4 Hz), 186.3 (2C), 184.1 (2C), 177.3 (1C), 175.6 (1C), 172.4 (1C), 172.1 (1C), 170.1 (1C) (pattern unchanged at –95 °C); MS (EI; *m/z*) 1196 [M]⁺. Anal. Calcd for C₂₉H₁₂F₃O₁₁Os₃P: C, 29.15; H, 1.01. Found: C, 29.35; H, 1.07. Os₃(CO)₁₁[P(C(CH₃)₃)₃]: mp 144.5–145.5 °C; UV–vis (hexane) 31 400 (ε_M × 10^{–4} = 7.91), 26 700 (6.49), 21 400 (5.66) cm^{–1}; IR (hexane) ν(CO) 2105.5 (m), 2055 (s), 2020 (vs), 2009 (m), 2002 (w), 1991.5 (vw), 1981 (w), 1944 (w), 1930 (w) cm^{–1}; ¹H NMR (CD₂Cl₂) δ 1.56 (d, *J*_{PH} = 12.5 Hz) (unchanged in CD₂Cl₂/CH₂Cl₂ at –120 °C); ³¹P{¹H} NMR (CD₂Cl₂) δ 80.6 (s, unchanged in CD₂Cl₂/CH₂Cl₂ at –120 °C); ¹³C{¹H} NMR (CD₂Cl₂/CH₂Cl₂ 1:4; –60 °C) δ 197.4 (2C, *J*_{PC} = 6.1 Hz), 185.5 (2C), 182.5, (2C), 175.9 (1C), 173.2 (1C), 171.7 (1C), 169.5 (1C); MS (EI; *m/z*) 1082 [M]⁺. Anal. Calcd for C₂₃H₂₇O₁₁Os₃P: C, 25.56; H, 2.52. Found: C, 25.69; H, 2.43.

X-ray Analyses of 1 and 2. The preparation of the crystals of the red and yellow forms of **1** is intriguing and hence is presented here in detail. To pure compound **1** (20 mg) was added (under nitrogen) hexane (10 mL) and the mixture refluxed until **1** had dissolved. The Schlenk flask with the solution was stored at –40 °C overnight. By this procedure, **1** was obtained as feather-like needles from which **1y1** was obtained. When a similar hot hexane solution of **1** was set aside at room temperature, besides the yellow feather-like crystals of **1** it yielded a few well-formed red blocks of **1r**. On standing overnight the red crystals apparently cannibalized the yellow form such that only red crystals remained. The yellow solution from one of these crystallizations was discarded to a Schlenk tube left open to the air in the fumehood where, upon evaporation of the solvent, yellow crystals of **1** were found that were visibly of superior quality than those resulting from previous (careful) crystallizations. From these crystals sample **1y** was obtained. Crystals of **2** were obtained by cooling a hot hexane solution of the compound at 6 °C. Two crystalline forms of **1y** were investigated designated as **1y** and **1y1**. All X-ray diffraction data for **1y**, **1y1**, **1r**, and **2** were collected on a Siemens SMART/CCD diffractometer equipped with an LT-II low-temperature device. The diffraction data were corrected for absorption by using the SADABS program. The program SHELXTL¹⁶ was used for the structure solution, and the refinement was based on *F*². The *p*-fluorophenyl groups of **1y1** were disordered, and the disorder could not be readily modeled. The refinement of this structure was therefore not pursued further. For the other structures, all the non-hydrogen atoms were refined anisotropically with the exception of four carbon atoms of **1y**, namely, C41, C64, C400, and C502, which gave negative temperature factors and were therefore refined isotropically. Hydrogen atoms were fixed in calculated posi-

(11) (a) Ang, H. G.; Kwik, W. L.; Leong, W. K.; Potenza, J. A. *Acta Crystallogr.* **1989**, C45, 1713. (b) Ang, H. G.; Cai, Y. M.; Kwik, W. L.; Leong, W. K.; Tocher, D. A. *Polyhedron* **1991**, 10, 881. (c) Ang, H.-G.; Cai, Y. M.; Kwik, W. L. *J. Organomet. Chem.* **1993**, 448, 219. (d) Ang, H. G.; Koh, C.-H.; Koh, L.-L.; Kwik, W.-L.; Leong, W.-K.; Leong, W.-Y. *J. Chem. Soc., Dalton Trans.* **1993**, 847. (e) Ang, H.-G.; Ang, S.-G.; Kwik, W.-L.; Zhang, Q. *J. Organomet. Chem.* **1995**, 485, C10. (f) Johnson, B. F. G.; Lewis, J.; Norlander, E.; Raithby, P. R. *J. Chem. Soc., Dalton Trans.* **1996**, 3825. (g) Bartsch, R.; Blake, A. J.; Johnson, B. F. G.; Jones, P. G.; Mueller, C.; Nixon, J. F.; Nowotny, M.; Schumtzer, R.; Shepherd, D. S. *Phosphorus, Sulfur, Silicon Relat. Elem.* **1996**, 115, 201. (f) Biradha, K.; Hansen, V. M.; Leong, W. K.; Pomeroy, R. K.; Zaworotko, M. J. *J. Clust. Sci.*, submitted for publication.

(12) (a) Bruce, M. I.; Liddel, M. J.; Hughes, C. A.; Patrick, J. M.; Skelton, B. W.; White, A. H. *J. Organomet. Chem.* **1988**, 347, 181. (b) Bruce, M. I.; Liddel, M. J.; bin Shawkataly, O.; Hughes, C. A.; Skelton, B. W.; White, A. H. *J. Organomet. Chem.* **1988**, 347, 207.

(13) Alex, R. F.; Einstein, F. W. B.; Jones, R. H.; Pomeroy, R. K. *Inorg. Chem.* **1987**, 26, 3175.

(14) Biradha, K.; Gilmour, B. S.; Hansen, V. M.; Ma, A. K.; Pomeroy, R. K.; Wong, E.; Zaworotko, M. J. Unpublished results. See also: Ma, A. K. Ph.D. Thesis, Simon Fraser University, 1992.

(15) (a) Johnson, B. F. G.; Lewis, J.; Pippard, D. A. *J. Chem. Soc., Dalton Trans.* **1981**, 407. (b) Nicholls, J. N.; Vargas, M. D. *Inorg. Synth.* **1990**, 28, 232.

(16) Sheldrick, G. M. *SHELXTL*; Siemens: Madison, WI, 1995.

Table 1. Crystal Data and Structure Refinement for Yellow and Red Os₃(CO)₁₁[P(*p*-C₆H₄F)₃] (**1y**, **1y**, **1r**) and Os₃(CO)₁₁(P*t*Bu₃) (**2**)

| | 1y | 1y | 1r | 2 |
|---------------------------------------|--|--|--|---|
| formula | C ₂₉ H ₁₂ F ₃ O ₁₁ Os ₃ P | C ₂₉ H ₁₂ F ₃ O ₁₁ Os ₃ P | C ₂₉ H ₁₂ F ₃ O ₁₁ Os ₃ P | C ₂₃ H ₂₇ O ₁₁ Os ₃ P |
| temp (K) | 193(2) | 183(2) | 193(2) | 183(2) |
| cryst syst | orthorhombic | triclinic | monoclinic | monoclinic |
| space group | <i>Pnma</i> | <i>P</i> $\bar{1}$ | <i>P</i> 2 ₁ / <i>n</i> | <i>P</i> 2 ₁ / <i>c</i> |
| <i>a</i> (Å) | 29.671(2) | 9.616(4) | 13.9258(7) | 17.0703(9) |
| <i>b</i> (Å) | 11.8805(6) | 12.873(6) | 12.2851(6) | 11.2941(6) |
| <i>c</i> (Å) | 10.1114(5) | 26.433(12) | 18.3017(10) | 17.3047(10) |
| α (deg) | 90 | 87.295(14) | 90 | 90 |
| β (deg) | 90 | 83.12(2) | 91.4040(10) | 119.1080(10) |
| γ (deg) | 90 | 69.26(2) | 90 | 90 |
| <i>V</i> (Å ³), <i>Z</i> | 3564.3(3), 4 | 3038(2), 4 | 3130.1(3), 4 | 2914.9(3), 4 |
| <i>D</i> (calcd) (Mg/m ³) | 2.227 | 2.613 | 2.536 | 2.463 |
| abs coeff (mm ⁻¹) | 10.781 | 12.648 | 12.276 | 13.153 |
| indpdtd reflns | 2708 [<i>R</i> (int) = 0.0465] | 10 507 [<i>R</i> (int) = 0.0536] | 4491 [<i>R</i> (int) = 0.0336] | 6822 [<i>R</i> (int) = 0.0339] |
| <i>R</i> _F ^a | 0.0931 | 0.0407 | 0.0271 | 0.0248 |
| <i>R</i> _{wF} ^b | 0.269 | 0.0891 | 0.0594 | 0.0533 |

^a *R*_F = $\sum(|F_o| - |F_c|)/\sum|F_o|$; *I*₀ = 2.0σ(*I*₀). ^b *R*_{wF} = $[\sum(w(|F_o| - |F_c|)^2)/\sum(wF_o^2)]^{1/2}$. *w* = $[\sigma^2(F_o) + kF_o^2]^{-1}$.

Table 2. Selected Bond Lengths (Å) and Angles (deg) for **1** and **2**

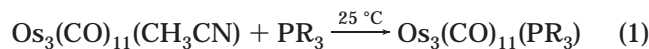
| | 1y | 1y ^a | 1r | 2 |
|---|-----------|------------------------|---------------------------------|---------------------------------|
| Os(1)–Os(2) | 2.886(2) | 2.859(1), 2.844(1) | 2.8835(4) | 2.9214(3) |
| Os(1)–Os(3) | 2.900(2) | 2.872(1), 2.888(1) | 2.9117(4) | 2.9416(3) |
| Os(2)–Os(3) | 2.878(2) | 2.859(1), 2.856(1) | 2.8654(4) | 2.8629(3) |
| Os(1)–P | 2.36(1) | 2.341(3), 2.331(3) | 2.353(2) | 2.478(1) |
| Os–C _{eq} (range) | | 1.85(2)–1.90(2) | 1.903(9)–1.926(9) | 1.857(5) ^b –1.918(5) |
| Os–C _{ax} (range) | | 1.91(1)–1.95(1) | 1.922(8)–1.95(1) | 1.928(5)–1.958(5) |
| Os–Os–Os (range) | | 59.37(3)–60.87(2) | 59.26(1)–60.86(1) | 58.455(6)–61.124(7) |
| P–Os(1)–C(13) | | 102.3(4), 99.3(3) | 98.7(2) | 92.45(13) |
| C _{eq} –Os–C _{eq} | | 100.8(5)–103.6(5) | 99.8(4), 103.5(4) | 98.5(2), 101.3(2) |
| C _{ax} –Os–C _{ax} (range) | | 173.8(6)–178.4(6) | 170.6(4) ^c –175.1(3) | 165.8(2) ^c –175.7(2) |

^a Two independent molecules in unit cell. ^b Os(1)–C(13). ^c C(11)–Os(1)–C(12).

tions and refined isotropically on the basis of the corresponding C atoms [*U*(H) = 1.2 *U*_{eq}(C)]. Pertinent crystallographic data are given in Table 1; selected bond length and angle data are given in Table 2. Fractional coordinates and anisotropic displacement parameters have been deposited as Supporting Information.

Results and Discussion

The clusters Os₃(CO)₁₁(PR₃) (R = *p*-C₆H₄F, **1**; R = Bu^t, **2**) were prepared by treatment of Os₃(CO)₁₁(CH₃CN) (eq 1) with PR₃, a standard protocol for the synthesis of Os₃-



(CO)₁₁(PR₃) compounds.^{6,15} As mentioned in the Introduction, we have synthesized over 20 compounds of this type by this method. Although no quantitative studies were carried out, it was noted that the rate of the reaction depended both on the size (cone angle) and donor properties of the PR₃ ligand employed. The syntheses of **1** and **2** partially illustrate this observation. The preparation of **1** was complete in 15 min, as indicated by IR spectroscopy, whereas that of **2** took 18 h; the cone angles of P(*p*-C₆H₄F)₃ and P*t*Bu₃ are 145° and 182°, respectively.¹⁷ The yield of **2** (~30%) was the lowest of the derivatives prepared. The Os₃(CO)₁₁(PR₃) derivatives are air stable crystalline solids that with the exceptions described here are yellow or orange.

In one preparation of **1** it was noticed that there were both yellow (**1y**) and red (**1r**) crystals present in the sample. Closer investigation revealed that when a hot hexane solution (with or without a small amount of CH₂Cl₂) of **1** was allowed to cool to room temperature, both red and yellow crystals formed. When this solution was allowed to stand, the red crystals became more numerous at the expense of the yellow crystals until after 24 h only red blocklike crystals remained. When hot hexane solutions of **1** were steadily cooled to -40 °C, only yellow crystals resulted. As such, the crystals were feather-like needles and mostly unsuitable for crystallographic study. A crystal (**1y1**) from this preparation was, however, found that diffracted, but the structure obtained from the diffraction data was partly disordered (see below). By chance, it was noticed that a sample of **1** in hexane that had been allowed to evaporate in air had yielded well-formed yellow crystals of **1** (**1y**). Crystallographic investigation of one of these crystals revealed it was yet another polymorph of the compound and, furthermore, was an ordered structure.

When **1y** was heated, it turned orange in the approximate range 70–110 °C and melted at essentially the same temperature as the red form. DTA of **1y** and **1r** exhibited peak maxima at 165.5 and 165.0 °C, respectively, with no evidence of any phase change up to the melting point for either polymorph.

Dissolution of **1r** in hexane gave yellow solutions with spectroscopic properties identical to those of hexane solutions of **1y**; when **1r** was dissolved in CH₂Cl₂ at -78 °C, the resulting solution was yellow. These observations suggest that the cause of the color change in **1** is

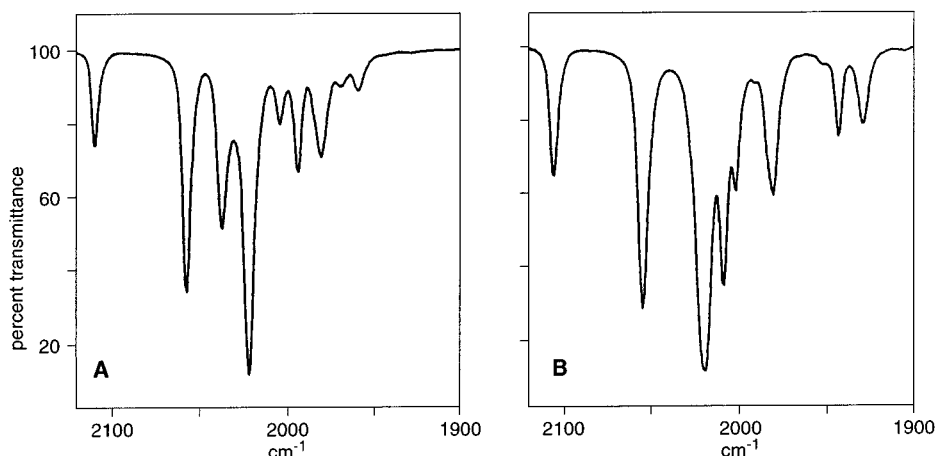


Figure 1. Infrared spectrum (CO-stretching region) of $\text{Os}_3(\text{CO})_{11}[\text{P}(p\text{-C}_6\text{H}_4\text{F})_3]$, **1**, (A) and $\text{Os}_3(\text{CO})_{11}(\text{PBu}_3)_3$, **2**, (B) in hexane.

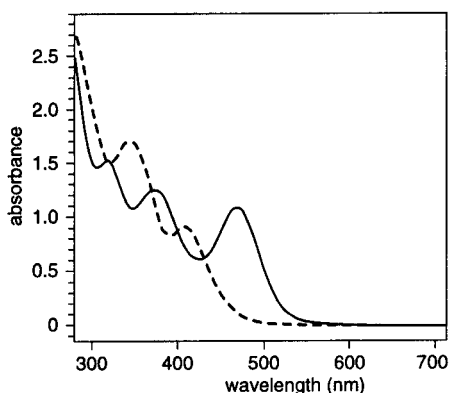


Figure 2. UV-vis spectrum of **1** (dotted line) and **2** (solid line) in hexane.

due to intermolecular forces (see below). The IR and ^{13}C NMR spectra of **1y** (CO region) are typical of the $\text{Os}_3(\text{CO})_{11}(\text{PR}_3)$ compounds that we have investigated; the IR spectrum of **1y** (CO stretching region) in hexane is shown in Figure 1.

Unlike the other $\text{Os}_3(\text{CO})_{11}(\text{PR}_3)$ compounds studied, **2** is deep red in solution and yields deep red, almost black, crystals when such solutions are cooled. The yellow or orange $\text{Os}_3(\text{CO})_{11}(\text{PR}_3)$ clusters have two weak absorptions in the UV-vis spectrum in the region $24\,000\text{--}32\,000\text{ cm}^{-1}$ that have been assigned in the parent $\text{Os}_3(\text{CO})_{12}$ cluster to σ to σ^* transitions involving molecular orbitals associated with the Os_3 unit;¹⁸ this is shown for **1y** in Figure 2. Cluster **2**, however, exhibits three bands in this region, at $31\,400$, $26\,700$, and $21\,400\text{ cm}^{-1}$ (Figure 2); the lowest energy bands absorb most of the green of the visible spectrum so that **2** is red. The maxima of the lowest energy band in both **1y** and $\text{Os}_3(\text{CO})_{11}(\text{PET}_3)$ ¹⁴ are around $24\,500\text{ cm}^{-1}$, which suggests that the band at $29\,900\text{ cm}^{-1}$ of **2** is also not due to the same electronic transition as in the other $\text{Os}_3(\text{CO})_{11}(\text{PR}_3)$ molecules. The UV-vis spectrum exhibited by **2** indicates its electronic structure is unique of the $\text{Os}_3(\text{CO})_{11}(\text{PR}_3)$ compounds so far investigated. We believe that this is strong evidence that **2** has a genuinely different conformation for an $\text{Os}_3(\text{CO})_{11}(\text{PR}_3)$ cluster and not just a more distorted version of the typical conformation. The

IR spectrum of **2** in the CO-stretching region is somewhat different from that of other $\text{Os}_3(\text{CO})_{11}(\text{PR}_3)$ complexes and is illustrated in Figure 1.

The ^{13}C NMR spectrum of **2** (^{13}C enriched) in $\text{CH}_2\text{Cl}_2/\text{CD}_2\text{Cl}_2$ at $-60\text{ }^\circ\text{C}$ exhibits three resonances of intensity 2 in the $182\text{--}198\text{ ppm}$ region assigned to the (pseudo) axial carbonyls and five resonances in the $168\text{--}180\text{ ppm}$ region of intensity 1 and assigned to the (pseudo) equatorial carbonyls. This is typical of $\text{Os}_3(\text{CO})_{11}(\text{PR}_3)$ complexes (at temperatures just above $-50\text{ }^\circ\text{C}$ selective carbonyl exchange occurs in these complexes, which causes the resonances to broaden and collapse into the baseline at different rates).^{14,19,20} Both the ^1H and $^{31}\text{P}\{^1\text{H}\}$ NMR spectra of **2** in $\text{CFHCl}_2/\text{CD}_2\text{Cl}_2$ at $-120\text{ }^\circ\text{C}$ consist of singlets (with phosphorus coupling in the case of the ^1H NMR resonance). Although this does not completely rule out that both the *E* and *S* (see below) forms of **2** are present in solution in rapid equilibrium, the NMR and IR evidence indicates that this is most unlikely; that is, there is only one form of **2** in solution responsible for the three bands in the UV-vis spectrum.

Structures of $\text{Os}_3(\text{CO})_{11}[\text{P}(p\text{-C}_6\text{H}_4\text{F})_3]$. Three X-ray structures of **1** were carried out: two of the yellow (**1y1**, **1y**) and one of the red form (**1r**). Selected bond lengths and angles for the structures of **1** are given in Table 2. The *p*-fluorophenyl rings of **1y1** were disordered and could not be readily modeled, and therefore only the OsP and OsOs distances for **1y1** are given in the table. Further discussion on the structure of the yellow polymorphs is restricted to **1y**, the ordered form; this version contains two independent molecules in the unit cell. The structure of **1y** is as expected, with the vectors that pass through a given Os atom and the axial carbonyls associated with it essentially orthogonal to the Os_3 plane; a view of molecule 1 of **1y** is given in Figure 3. This geometry based on the D_{3h} structure of $\text{Os}_3(\text{CO})_{12}$ (Chart 1) we designate as “*E*” (eclipsed or erect). The range of the Os–Os bond lengths in the two independent molecules of **1y** is $2.844(1)\text{--}2.888(1)\text{ \AA}$. The average bond length in $\text{Os}_3(\text{CO})_{12}$ is $2.877(3)\text{ \AA}$,² whereas the Os–Os distances in $\text{Os}_3(\text{CO})_{11}(\text{PPh}_3)$ range from 2.886 to $2.918(1)\text{ \AA}$.⁸ As is generally observed in $\text{Os}_3(\text{CO})_{11}(\text{PR}_3)$ clusters,^{6,8–11} the longest Os–Os bond is

(18) (a) Tyler, D. R.; Levensen, R. A.; Gray, H. B. *J. Am. Chem. Soc.* **1978**, *100*, 7888. (b) Tyler, D. R.; Altobelli, M.; Gray, H. B. *J. Am. Chem. Soc.* **1980**, *102*, 3022.

(19) Johnson, B. F. G.; Lewis, J.; Reichert, B. E.; Schorpp, K. T. *J. Chem. Soc., Dalton Trans.* **1976**, 1403.

(20) Alex, R. F.; Pomeroy, R. K. *Organometallics* **1987**, *6*, 2437.

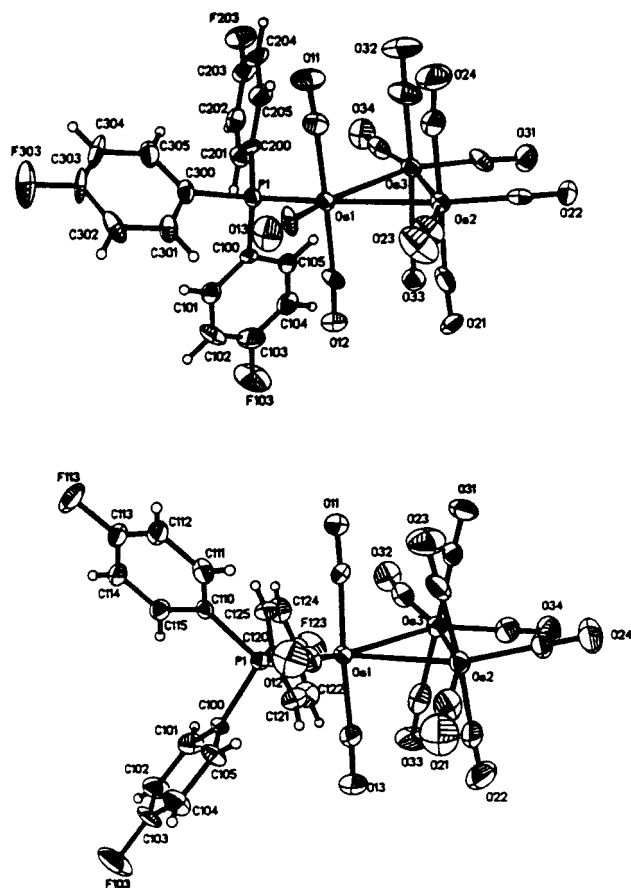


Figure 3. Molecular structure of the yellow (top) and red forms of $\text{Os}_3(\text{CO})_{11}[\text{P}(p\text{-C}_6\text{H}_4\text{F})_3]$ (**1y** and **1r**, respectively).

that which is cis to the phosphorus-donor ligand (i.e., $\text{Os}(1)\text{--Os}(3)$), although this lengthening is chemically not significant in **1y**.

The structure of **1r** is also depicted in Figure 3. It is immediately apparent that the structure is based on the D_3 form of $\text{Os}_3(\text{CO})_{12}$ (Chart 1) with the $\text{Os}(\text{CO})_4$ units twisted with respect to each other. We designate this conformer as "S" (staggered or slanted). The extent of this twisting can be measured in a number of ways; we have chosen to take the absolute value of the dihedral angle between the $\text{C}_{\text{ax}}\text{--Os}(2)\text{--C}_{\text{ax}}\text{--Os}(3)$ and $\text{C}_{\text{ax}}\text{--Os}(3)\text{--C}_{\text{ax}}\text{--Os}(2)$ planes of the $\text{Os}_2(\text{CO})_8$ fragment of the $\text{Os}_3(\text{CO})_{11}(\text{PR}_3)$ cluster. In this way the direct steric and electron effects of the PR_3 ligand are avoided (cf. the structure of **2** discussed below). This angle can range from 0° , as in the ideal form of the parent carbonyl $\text{Os}_3(\text{CO})_{12}$ with D_{3h} symmetry, to 45° . In **1r** this dihedral angle (i.e., that between the $\text{C}(22)\text{Os}(2)\text{C}(23)\text{Os}(3)$ and $\text{C}(31)\text{Os}(3)\text{C}(33)\text{Os}(2)$ planes) is 24.5° . (The $\text{C}_{\text{ax}}\text{--Os}(2)\text{--Os}(3)\text{--C}_{\text{ax}}$ dihedral angles used by Bruce and co-workers to describe this twisting are 23.1° and 26.1° .) The corresponding angle for **1y** is 2.0° in both of the independent molecules. The distances between the pseudoaxial carbonyl on one osmium atom to the next closest osmium atom (e.g., $\text{Os}(1)\cdots\text{C}(23)$) are in the range $3.07(1)\text{--}3.26(1)$ Å and cannot be considered as semibringing interactions. In **1y** these distances are in the range $3.32(1)\text{--}3.50(1)$ Å.

The $\text{Os}\text{--Os}$ bond cis to the P-donor ligand in **1r** ($2.912(1)$ Å) and that trans to this ligand ($2.884(1)$ Å) are lengthened compared to the corresponding distances

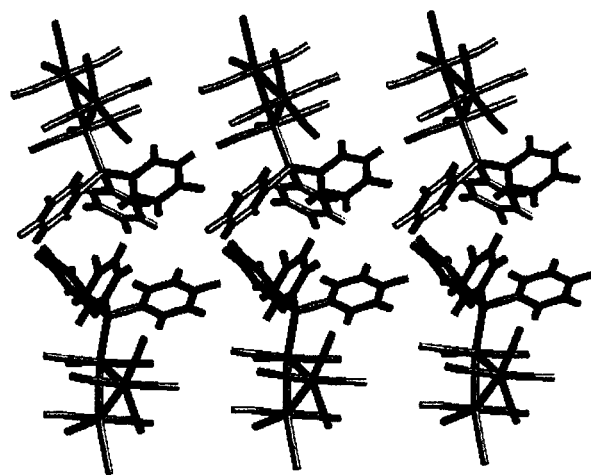


Figure 4. Partial packing diagram for **1y** showing the edge-to-face interactions of the p -fluorophenyl rings.

in **1y** (2.877 , $2.888(1)$, and 2.859 , $2.844(1)$ Å, respectively). These lengths suggest that the metal–metal bonds in **1r** are somewhat weaker than those in **1y**, which is therefore consistent with the view that in the S form of $\text{M}_3(\text{CO})_{12}$ there is less metal–metal bonding than in the E form.³

The question naturally arises as to the origin of the twisting in the red isomer of **1**. The steric and σ -donor/ π -acceptor properties of the $\text{P}(p\text{-C}_6\text{H}_4\text{F})_3$ ligand lie approximately in midrange for common P ligands: the cone angle of the ligand is 145° , and the Tolman electronic parameter 2071.3 cm^{-1} .¹⁷ It appears unlikely, therefore, that the stability of the S form of **1** can be attributed to any unusual steric or donor properties of the $\text{P}(p\text{-C}_6\text{H}_4\text{F})_3$ ligand. It is known, however, that phenyl groups of molecules or ions pack effectively, with specific geometries, so as to lead to solids that have high crystallinity and low solubility.²¹ For example, recent studies have described structures with $[\text{Ph}_4\text{P}]^+$ cations which contain one-dimensional supramolecular motifs that involve concerted, multiple phenyl embraces based on edge-to-face interactions between phenyl groups of different $[\text{Ph}_4\text{P}]^+$ cations.^{22a} In **1y** each $\text{P}(p\text{-C}_6\text{H}_4\text{F})_3$ group forms a sextuple embrace with a second $\text{P}(p\text{-C}_6\text{H}_4\text{F})_3$ group through such aromatic edge-to-face interactions.^{22b} These aggregates pack in the y -direction also via edge-to-face binding (Figure 4). On the other hand, in **1r** the $\text{P}(p\text{-C}_6\text{H}_4\text{F})_3$ ligands do not form a sextuple embrace, but rather the phenyl rings of one $\text{P}(p\text{-C}_6\text{H}_4\text{F})_3$ substituent interacts with the phenyl rings of its two nearest neighbors by four edge-to-face interactions to give a one-dimensional chain (Figure 5).²³ We believe that these interactions are responsible for the twisting of Os_3 framework in **1r**. As mentioned previously, that **1r** reverts to the yellow form on dissolution in CH_2Cl_2 or hexane suggests that it is an intermolecular interaction in the solid state that is the cause of the distortion in **1r**. The presence of the electronegative

(21) Dance, I. G.; In *Perspectives in Supramolecular Chemistry: The Crystal as a Supramolecular Entity*; Desiraju, G. R., Ed.; Wiley: Chichester, 1996; Vol. 2.

(22) (a) Dance, I. G.; Scudder, M. J. *Chem. Soc., Dalton Trans.* **1996**, 3755. (b) Dance, I. G.; Scudder, M. J. *Chem. Soc., Chem. Commun.* **1995**, 1039.

(23) Note the conversion of **1y** to **1r** would involve a small displacement in the y -direction of one row of molecules with respect to the adjacent row.

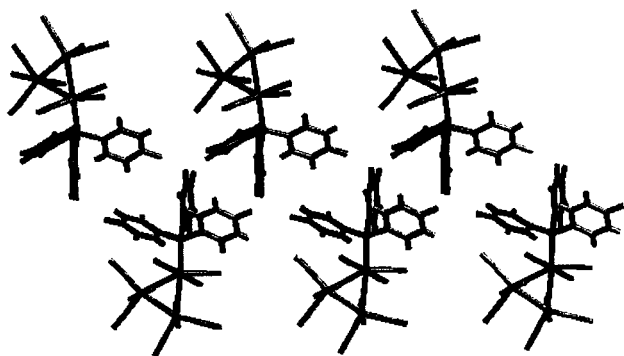


Figure 5. Partial packing diagram for **1r**.

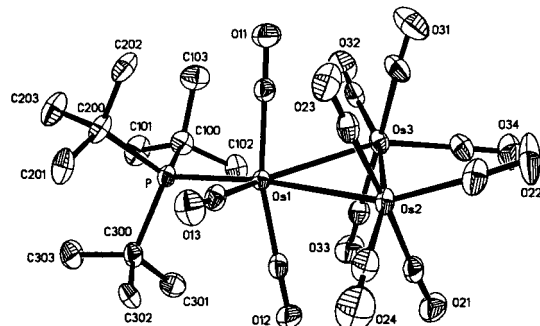


Figure 6. Molecular structure of **2**.

fluorine atom would be expected to lower the energy of the acceptor π^* MO of the fluorophenyl ring and could lead to these interactions being stronger than in say $\text{Os}_3(\text{CO})_{11}(\text{PPh}_3)$. The perfluorophenyl derivative $\text{Os}_3(\text{CO})_{11}[\text{P}(\text{C}_6\text{F}_5)_3]$ has the *E* configuration,^{11a} and we found no evidence for a red form in our spectroscopic investigation of this cluster.

In **1r** an oxygen atom of one of the pseudoaxial CO ligands (i.e., O(33)) makes close approach (3.13(1) Å) to the plane of one of fluorophenyl rings (ring 2; Figure 3), which might indicate a weak bonding interaction arising from electron donation from the π MO on the CO ligand to the π^* MO of the fluorophenyl ring. (Electron donation from groups other than CO to phenyl rings has been proposed to occur in biochemical molecules.)²⁴ Molecular orbital calculations (ab initio with a 3-12G** basis set), however, based on distances and angles found in **1r** did not indicate any significant interaction between a carbonyl group and fluorobenzene.

Structure of $\text{Os}_3(\text{CO})_{11}(\text{PBUt}_3)$. The structure of **2** is shown in Figure 6; as can be seen from the figure, it too has the twisted *S* conformation. The dihedral angle between the $\text{C}_{\text{ax}}\text{--Os--C}_{\text{ax}}\text{--Os}$ planes of the $\text{Os}_2(\text{CO})_8$ grouping in **2** is 32.9° ($\text{C}_{\text{ax}}\text{--Os(2)--Os(3)--C}_{\text{ax}}$ dihedral angles of 32.4° and 33.8°). The distances between the pseudoaxial carbonyls and the nearest nonbonded osmium atom are in the range 3.05(1)–3.20(1) Å and as in **1r** do not indicate any significant bonding interaction. The Os–Os bond cis to the phosphine ligand in **2** is, at 2.9416(3) Å, among the longest Os–Os bonds reported for $\text{Os}_3(\text{CO})_{11}(\text{PR}_3)$ compounds. In $\text{Os}_3(\text{CO})_{11}[\text{PBUt}_2(\text{NH}_2)]$ the corresponding length is 2.953(1) Å in one of

the two independent molecules in the unit cell;⁹ in $\text{Os}_3(\text{CO})_{11}[\text{P}(o\text{-C}_6\text{H}_4\text{Me})_3]$ the Os–Os bond cis to the P-donor ligand has a length of 2.9429(4) Å.^{11f} The lengthening of the metal–metal bond cis to the PBUt_3 ligand in **2** can be attributed to both steric and electronic factors. It has previously been found that as the cone angle of PR_3 increases, the cis Os–Os distance in $\text{Os}_3(\text{CO})_{11}(\text{PR}_3)$ compounds increases.⁸ In unpublished work we have found that for $\text{Os}_3(\text{CO})_{11}[\text{P}(\text{OPh})_3]$ the cis Os–Os length is 2.8941(6) Å, whereas in the PET_3 analogue the corresponding length is 2.9242(4) Å.^{11f} The cone angles of the phosphite (128°) and of the phosphine (132°) are approximately equal, whereas their donor properties are significantly different (Tolman electronic parameters of 2085.3 and 2061.7 cm^{-1} , respectively).¹⁷ The increase in the Os–Os distance in the PET_3 compound therefore indicates that the σ -donor/ π -acceptor properties of the P ligand also influence the cis Os–Os length; that is, better donor ligands lengthen the cis Os–Os bond. The PET_3 and PBUt_3 ligands have similar donor properties (Tolman parameters of 2061.7 and 2056.1 cm^{-1} , respectively). It could be argued, therefore, that steric interactions in **2** are responsible for an increase of approximately 0.2 Å in the cis Os–Os length in **2**. The Os–Os distance trans to the PBUt_3 ligand in **2** is 2.9214(3) Å, which is the longest Os–Os bond of this type yet reported for $\text{Os}_3(\text{CO})_{11}(\text{PR}_3)$ complexes, an observation that can undoubtedly be attributed to the strong σ -donor properties of PBUt_3 (see below). The remaining Os–Os bond length in **2** is 2.8629(3) Å. Structures of $\text{Os}_3(\text{CO})_{11}(\text{PR}_3)$ compounds reveal, not unexpectedly, that the length of this Os–Os bond is insensitive to the nature of R.^{7–12}

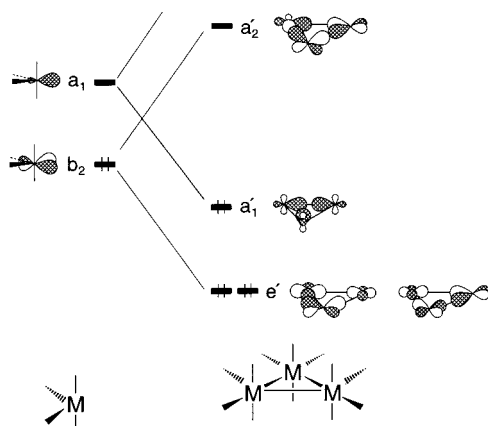
There are two additional features of interest in the structure of **2**. The Os–P length of 2.478(1) Å in **2** is by far the longest Os–P bond length for an $\text{Os}_3(\text{CO})_{11}(\text{PR}_3)$ cluster previously reported or determined in this laboratory.^{7–12,14} For example, the Os–P lengths in **1y**, **1r**, and $\text{Os}_3(\text{CO})_{11}(\text{PET}_3)$ are 2.331(3) and 2.341(3), 2.353(2), and 2.345(2) Å, respectively.^{11f} Given that the PET_3 and PBUt_3 ligands have similar donor properties, the lengthening of the Os–P bond in **2** can be attributed to steric effects of the large PBUt_3 ligand (cone angle = 182°).¹⁷ That the pseudoaxial carbonyl ligands bound to the same Os atom as the PBUt_3 substituent are bent away from this group by some 10° from the angle expected for octahedral geometry (Table 2) is consistent with this view. The second noteworthy aspect of **2** is that the angle the equatorial ligands make at Os(1) (i.e., C(13)Os(1)P(1)) is 92.5(1)°, whereas the other angles of this type in **2** and those in **1y** and **1r** are in the range 98.5(1)–103.6(5)°.

Unlike $\text{P}(p\text{-C}_6\text{H}_4\text{F})_3$, PBUt_3 is an exceptional ligand. It is the strongest σ -donor of the common phosphorus ligands (the Tolman electronic parameter for PBUt_3 is 2056.1 cm^{-1}); it also has one of the largest cone angles ($\theta = 182^\circ$) of the PR_3 class of ligands.¹⁷ We believe that these exceptional properties are responsible for the *S* conformation adopted in **2**.

The metal–metal bonding in $\text{M}_3(\text{CO})_{12}$ is often described in terms of localized 2c–2e bonds of octahedral $\text{M}(\text{CO})_4$ fragments. What is believed to be a more correct description of the bonding in the M_3 core, however, is one that involves a central MO resulting

(24) (a) Burley, S. K.; Petsko, G. A. *Adv. Protein Chem.* **1988**, *39*, 125. (b) Waksman, G.; Kominos, D.; Robertson, S. C.; Pant, N.; Baltimore, D.; Birge, R. B.; Cowburn, D.; Hanafusa, H.; Mayer, B. J.; Overduin, M.; Resh, M. D.; Rios, C. B.; Silverman, L.; Kuriyan, J. *Nature* **1992**, *358*, 646.

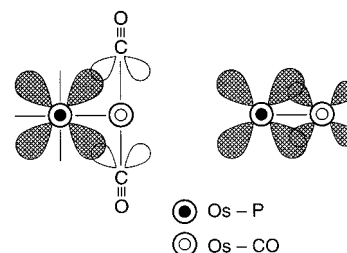
Chart 2



from the overlap of atomic orbitals on the individual M atoms, plus a lower energy pair of molecular orbitals that involve overlap of atomic orbitals along the edges of the M_3 triangle.^{4,5} (Recall that an $M(CO)_4$ fragment is isolobal with CH_2 with a_1 and b_1 frontier orbitals.)²⁵ This is shown in Chart 2 (adapted from that in ref 4). Lengthening the M–M vectors, as in **2**, would decrease these overlaps especially along the edges of the metal triangle. As mentioned in the Introduction, it is believed that these edge-bridging MOs are responsible for the D_{3h} conformation of $M_3(CO)_{12}$.³ We believe that in **2** the bonding contribution of these edge MOs has been reduced such that the D_3 form is preferred for steric reasons. The presence of three transitions in the UV–vis spectrum implies that in **2** the e' set of molecular orbitals has been split, with perhaps one of the resulting molecular orbitals higher in energy than the a_1' MO. In $(OC)_5M'[Os(CO)_3(PMe_3)]_2$ ($M' = Cr, Mo, W$) clusters which contain an $M'Os_2$ triangle, the radial carbonyls on the $M'(CO)_5$ unit are staggered with respect to the axial carbonyl groups on the Os atoms. It is thought that the main bonding interaction of the group 6 metal atom to the Os_2 fragment is via a single 3c–2e MO (the $M'(CO)_5$ fragment is isolobal with CH_3 with a single frontier MO). Interestingly, the $(OC)_5M'[Os(CO)_3(PMe_3)]_2$ clusters are, like **2**, deep red.²⁶

Simple lengthening of the Os–Os edges cannot be the complete explanation as to why **2** has the twisted S conformation since, as mentioned above, the cis Os–Os length in $Os_3(CO)_{11}[P(o-C_6H_4Me)_3]$ is longer than that in **2**, but the $P(o-C_6H_4Me)_3$ derivative has the E structure.^{11f} The cone angle of $P(o-C_6H_4Me)_3$ (194°) is larger than that of PBu^t_3 .¹⁷ It is found that the barrier to CO exchange in $Os_3(CO)_{11}(PR_3)$ is significantly lowered to that in the parent $Os_3(CO)_{12}$.^{14,19,20} To rationalize this observation, we have proposed that the better donor PR_3 ligand increases the electron density at the Os atom of the $Os(CO)_3(PR_3)$ unit in $Os_3(CO)_{11}(PR_3)$ compared to the Os atoms of the $Os(CO)_4$ groupings in $Os_3(CO)_{12}$. This in turn expands the filled 5d orbitals on the unique Os atom and allows better overlap with the π^* MO of the axial carbonyls on the neighboring Os atoms, thereby lowering the activation energy needed to form the CO-bridged intermediate necessary for carbonyl

Chart 3



exchange to take place (Chart 3).²⁰ If such an explanation is correct, then expansion of the 5d orbitals on the Os atom of the $Os(CO)_3(PR_3)$ grouping would also cause an increased interaction with the corresponding filled 5d orbitals on the other Os atoms in the cluster; this is also shown in Chart 3. Such an interaction would be repulsive and lead to a lengthening of the cis Os–Os bond with increased donor ability of the PR_3 ligand, as observed. (Consistent with this proposal is that **2** has one of the lowest barriers to axial–equatorial, merry-go-round CO exchange, and that the lowest-energy exchange takes place across the long cis Os–Os bond.)¹⁴ Twisting of the $Os(CO)_3(L)$ ($L = CO, PBu^t_3$) groups might be expected to reduce this repulsive interaction and hence would also favor the S conformation as adopted by **2**. The donor properties of $P(o-C_6H_4Me)_3$ are somewhat less than those of PBu^t_3 (Tolman parameters of 2066.6 and 2056.1 cm^{-1} , respectively)¹⁷ and might account for why the E conformation is maintained in $Os_3(CO)_{11}[P(o-C_6H_4Me)_3]$. (The structure of $Os_3(CO)_{11}(PCy_3)$ shows it has the common E conformation consistent with its UV–vis spectrum.)^{11f}

Conclusions

Deeming, in a review of substituted derivatives of $M_3(CO)_{12}$ ($M = Ru, Os$) with ligands coordinated only through heteroatoms, has pointed out that clusters of the type $M_3(CO)_{11}(L)$ are based on the parent carbonyl with either equatorial L (for $L = P-, As-, S-$ donor ligand, etc.) or axial L ($L = MeCN, Bu^tNC, NH=C(CH_2)_5$).⁶ It is only in the more highly substituted derivatives such as $Ru_3(CO)_8(L)_4$ ($L = P(OMe)_2Ph, PMe_2Ph, P(OMe)_3$) that distorted structures with semibridging carbonyls, similar to the structure of $Fe_3(CO)_{12}$, are observed.²⁷ For the mixed metal derivative $FeRu_2(CO)_{10}(PPh_3)_2$ a third structural form is observed in which two of the carbonyl ligands have semibridging interactions across different Ru–Fe bonds.²⁸ As mentioned in the Introduction, although distortions from E toward the S geometry are observed in some solid-state structures of $M_3(CO)_{11}(L)$ clusters, the distortions are generally small. In the more highly substituted clusters, however, the S geometry is more common. In $Os_3(CO)_6[P(OMe)_3]_6$ (also prepared in this laboratory) there is significant distortion toward the S conformer and there are no semibridging CO contacts. The distortion in this compound, however, can undoubtedly be attributed to the minimization of the steric interactions

(25) Hoffmann, R. *Angew. Chem., Int. Ed. Engl.* **1982**, 21, 711.

(26) Batchelor, R. J.; Davis, H. B.; Einstein, F. W. B. E.; Johnston, V. J.; Jones, R. H.; Pomeroy, R. K.; Ramos, A. F. *Organometallics* **1992**, 11, 3555.

(27) (a) Bruce, M. I.; Matison, J. G.; Patrick, J. M.; White, A. H.; Willis, A. C. *J. Chem. Soc., Dalton Trans.* **1985**, 1223. (b) Bruce, M. I.; Liddel, M. J.; bin Shawkataly, O.; Bytheway, I. Skelton, B. W.; White, A. H. *J. Organomet. Chem.* **1989**, 369, 217.

(28) Venäläinen, T.; Pakkanen, T. *J. Organomet. Chem.* **1984**, 266, 269.

between the bulky phosphite ligands that occupy all the equatorial sites in the molecule. Interestingly, the $\text{Os}_3(\text{CO})_6[\text{P}(\text{OMe})_3]_6$ cluster is orange-red with three absorptions in the UV-vis spectrum. It is, however, not as deeply colored as **2**.¹³

In this study, we have described two simple $\text{Os}_3(\text{CO})_{11}(\text{L})$ derivatives that have the twisted (*S*) rather than the previously observed *E* conformation. We believe that in **1r** ($\text{L} = \text{P}(p\text{-C}_6\text{H}_4\text{F})_3$) the twisting is the result of weak intermolecular bonding between the fluorophenyl rings in the solid state, that is, due to a bonding interaction that does not involve the metal skeleton. That the yellow form of **1** has the common *E* geometry with eclipsed adjacent carbonyl ligands indicates the extrinsic bonding interaction in **1r** is weak; the solution properties of **1** are consistent with only the presence of the *E* conformation in solution. The *S* configuration is also found for **2** ($\text{L} = \text{P}^t\text{Bu}_3$) both in the solid state and in solution. We believe that the conformation of **2** is the result of both the exceptional σ -donor and steric properties of the P^tBu_3 ligand which destabilize the peripheral Os–Os bonding in the Os_3 skeleton so that the sterically preferred *S* conformer is favored. These results provide support of the theoretical study of Lauher, who found that the *S* conformation of $\text{Ru}_3(\text{CO})_{12}$ is only some 3 kcal mol^{−1} higher in energy than the *E* form.³

It is interesting that Bruce and co-workers found that distortion toward the *S* conformer was more prevalent in the structures of $\text{Ru}_3(\text{CO})_{11}(\text{PR}_3)$ compounds than their Os analogues, consistent with the weaker metal–metal bonding in the second-row derivative. (We have been unsuccessful in attempts to prepare the Ru congener of **2**.) It should, however, be mentioned that the $\text{C}_{\text{ax}}\text{--Os}(2)\text{--Os}(3)\text{--C}_{\text{ax}}$ angles for $\text{Ru}_3(\text{CO})_{11}(\text{PCy}_3)$ (3.7°, 4.7°) are much smaller than those in $\text{Ru}_3(\text{CO})_{11}$ –

$[\text{P}(\text{OCH}_2)_3\text{CET}]$ (22.5°, 24.4°),⁸ which is not expected from the arguments presented here but might be due to packing effects. On the other hand, the same workers found that the $\text{C}_{\text{ax}}\text{--Os}(2)\text{--Os}(3)\text{--C}_{\text{ax}}$ angles in $\text{M}_3(\text{CO})_{12-x}(\text{PR}_3)_x$ ($x = 2, 3$) were much larger than in the monosubstituted analogues,¹² which may be rationalized with arguments presented above.

It is known that large basic phosphine ligands can stabilize unusual bonding modes or electron configurations, for example, the $\eta^2\text{-H}_2$ complex $\text{W}(\text{CO})_3(\text{PPr}^i_3)_2(\eta^2\text{-H}_2)$ and the 17e compound $\text{Re}(\text{CO})_3(\text{PCy}_3)_2$.^{29,30} Recently, the first Ru_3 cluster with a 44e configuration, $\text{Ru}_3(\mu_3\text{-H})_2(\mu\text{-CO})_3(\text{CO})_3(\text{PCy}_3)_3$, has been described in which the tricyclohexylphosphine ligands are undoubtedly crucial to its stability.³¹ The synthesis and structure of **2** demonstrate that a large basic phosphine ligand can also distort the geometry of a simple metal carbonyl cluster compound.

Acknowledgment. We thank the Natural Sciences and Engineering Research Council of Canada and St. Mary's University for financial support. We also thank Dr. Noham Weinberg for the MO calculations.

Supporting Information Available: Figure of the molecular structure of **1y1**; listing of atomic coordinates, bond lengths and angles, anisotropic thermal parameters, and hydrogen atom coordinates for compounds **1y**, **1y1**, **1r**, and **2** (31 pages). Ordering information and Internet access instructions are given on any current masthead page.

OM980365G

(29) Kubas, G. J.; Ryan, R. R.; Swanson, B. I.; Vergamini, P. J.; Wasserman, H. J. *J. Am. Chem. Soc.* **1984**, *106*, 451.

(30) Walker, H. W.; Rattinger, G. B.; Belford, R. L.; Brown, T. L. *Organometallics* **1983**, *2*, 775.

(31) Süss-Fink, G.; Godefroy, I.; Ferrand, V.; Neels, A.; Stoeckli-Evans, H. *J. Chem. Soc., Dalton Trans.* **1998**, 515.